Primljen / Received: 23.1.2021.
Ispravljen / Corrected: 10.5.2020.
Prihvaćen / Accepted: 24.6.2020.
Dostupno online / Available online: 10.12.2022.

Pushover analysis for estimating seismic demand of elliptic braced moment resisting frames

Authors:

Research Assist. **Habib Ghasemi Jouneghani**
University of Technology Sydney, NSW, Australia
Faculty of Civil and Environmental Engineering
Habib.GhasemiJouneghani@uts.edu.au
Corresponding author

Assoc.Prof. **Abbas Haghollahi**, Ph.D. CE
Shahid Rajaee Teacher Training University
Teheran, Iran
Department of Civil Engineering
Haghollahi@Sru.ac.ir

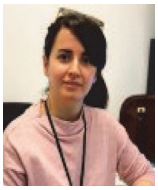

Lecturer **Mina Mortazavi**, Ph.D. CE
University of Technology Sydney, NSW, Australia
Faculty of Civil and Environmental Engineering
Mina.Mortazavi@uts.edu.au

Research Paper

Habib Ghasemi Jouneghani, Abbas Haghollahi, Mina Mortazavi

Pushover analysis for estimating seismic demand of elliptic braced moment resisting frames

In this paper, an innovative steel bracing system, known as the seismic response of elliptic braced moment resisting frame (ELBRF), is evaluated. ELBRF has a better structural behavior comparing to the other bracing systems and it has an architectural advantage allowing to place openings in walls with less interference. The demand for seismic performance of ELBRF is estimated through different loading patterns by adopting the conventional pushover methods. The pushover results are verified through nonlinear time history analysis (NTHAs) of 3, 5, 7, and 10-story ELBRF frames, which are on type II soil and are affected by 10 scaled earthquake records. These results are also with special moment resisting frames (SMRF) and X-Braced CBF and Inverted V-Braced CBF concentrically braced frames. Story drifts, displacements, and story shears are evaluated. A proportionally accurate estimation is observed through the pushover methods in comparison with NTHAs. Modal Pushover Analysis (MPA) can estimate the seismic demands by overcoming the shortcomings of FEMA load distributions when the higher mode effects are of concern. The seismic performance of the ELBRF system against earthquakes has improved, failure is transmitted to the upper stories, and the response modification factor is increased in ELBRF.

Key words:

elliptic braced moment resisting frame, seismic demand, nonlinear static pushover analysis, seismic performance, nonlinear time history analysis, response modification factor

Prethodno priopćenje

Habib Ghasemi Jouneghani, Abbas Haghollahi, Mina Mortazavi

Analiza postupnog guranja za procjenu seizmičkih zahtjeva okvira s eliptičnim vezovima

U ovom se radu vrednuje seizmički odziv inovativnog čeličnog veznog sustava: okvir s eliptičnim vezovima (elliptic braced moment resisting frames - ELBRF). ELBRF ima bolje konstrukcijsko ponašanje u odnosu na druge vezne sustave te arhitektonsku prednost koja smanjuje smetnje pri umetanju otvora u zidove. Seizmičko ponašanje ELBRF-a procjenjuje se pomoću različitih obrazaca opterećenja primjenom konvencionalne metode postupnog guranja konstrukcije. Rezultati analize potvrđuju se pomoću nelinearne analize primjenom vremenskog zapisa (nonlinear time history analysis - NTHA) ELBRF okvira na 3, 5, 7 i 10 katova na tlu 2. tipa pogođenih potresima magnitude do 10 i uspoređuju se s posebnim okvirima (special moment resisting frames - SMRF) i okvirima s križnim i obrnutim V centričnim vezovima. Vrednuju se međukatni pomaci, pomaci te katni posmici. Postiže se proporcionalno točno vrednovanje pomoću metoda postupnog guranja konstrukcije u usporedbi s NTHA-om. Modalna metoda postupnog guranja konstrukcije (MPA) omogućuje procjenu seizmičkih zahtjeva s ciljem prevladavanja nedostataka raspoređivanja opterećenja prema FEMA-i kada se radi o učincima viših modova. Poboljšano je seizmičko ponašanje protupotresnog sustava ELBRF, oštećenja se prenose na gornje katove, a povećava se i faktor modifikacije odziva kod ELBRF-ova.

Ključne riječi:
okvir s eliptičnim vezom, seizmički zahtjev, nelinearna statička analiza postupnog guranja, seizmičko ponašanje, nelinearna analiza primjenom vremenskog zapisa, faktor modifikacije odziva

1. Introduction

Studying the destruction of buildings during seismic events reveals that the conventional elastic methods are ineffective in design building. Such methods do not provide a real insight on how structures behave when exposed to the extreme seismic phenomenon. The real performance of structures is determined through performance-oriented methods and guidelines that are subject to a new outstanding design approach named performance-based design [1].

This new analytical design method has two major differences in relative to the conventional perspectives of earthquake engineering: first is the existence of a direct connection between design and structural performance, and second is it being multiple functional. The performance targets may be a stress level that shouldn't exceed a load, a displacement, a limit state or a target damage state. Most structural damage during earthquake ground motions are primarily produced by lateral displacements, which its estimation is important in the performance-based earthquake resistant design. The nonlinear time history analysis on an exact analytical model is the most adequate analysis in estimating the deformation. However, there exist many uncertainties regarding site-specific input generation and the common analytical models applied in representing structural behavior. Therefore, it is safer to be aware of having a simpler tool for analysing the seismic performance of a frame structure [2].

Prediction in assessing the performance of the structure exposed to the earthquake is made through a nonlinear time history analysis (NTHAs). The nonlinear dynamical method is the most embodied analysis method, which accepts a combination of ground motion records along with a precise structural model. Nonetheless, this method has a relatively low uncertainty. Calculated responses are very sensitive to the unique features of earth motion as to the used seismic inputs. Therefore, several analyses are required for the use of various ground motion records [3]. Although NTHAs results are commonly applied in theoretical studies, it is time-consuming and often difficult to be applied in designing, but worth applying a simple analysis method to evaluate the structure's seismic performance. Simple and cost-effective NSPAs is the appropriate method for this purpose as it delivers primary information , rather than running dynamic analysis.

In (NSP) or pushover analysis in NEHRP guidelines [4, 5], requirements are calculated through static nonlinear analysis of a structure subjected to its steady increase in lateral forces, and an invariant constant elevation distribution, to the extent where a particular point's displacement (control point) either reaches a specified target displacement rate or causes structure collapse. It is assumed that force distribution and target displacement are both subject to the response being controlled by a fundamental mode assumption. These latter states that the mode shape does not change after the structure yields, hence these assumptions are considered as approximations after the structure yields. Consequently, deformation estimates obtained from a pushover analysis may be inaccurate for structures where higher mode effects and the story shear forces are of concern.

The correlation between the story drift and the applied load pattern is sensitive [1, 6]. The essential requirement for pushover analysis is to choose the appropriate lateral load pattern since it represents the distribution of the inertial force at the structure height which is inflicted during the earthquake. Selecting a more proportional model that resembles to inertial forces distribution would yield better results in analyses [7]. To overcome these limitations, several researchers have proposed adaptive force distributions that attempt to follow the time-variant distributions of inertia forces [8-10]. While these latter may provide better estimates of seismic demands, they are conceptually complicated and computationally demanding for routine application in structural engineering practice.

In this study, the Structures Seismic Design Regulations (Standard No. 2800) [11] and Iranian National Building code (Part 10) [12] constitute the guidelines in steel structures' design. Both, the nonlinear static pushover and nonlinear dynamic time history analyses are performed in accomplishing the objectives. The new lateral load ELBRF system is analysed through these methods and according to its performance, the ELBRF is of more advantageous as opposed to other structural systems. Attempt is made here to first evaluate the seismic performance of ELBRF system in accordance with FEMA-356 load patterns (2000) [5], next, to analyse a pushover modal and the nonlinear time history subject to various earthquake records and then, compare this performance with other structural systems, like (SMRF), X-Braced CBF and Inverted V-Braced CBF.

The results obtained from running NSPA and NTHAs analyses consist of stories drifts, displacements, and shears. The accuracy of nonlinear static pushover analysis (NSPA) is assessed for estimating seismic deformation of structures as well. It is revealed that in a high-rise structure, the pushover analysis can never replace the time history analysis. The validity of ELBRF models' results is assessed through the nonlinear dynamic analysis of 3, 5, 7, and 10-story ELBRF subject to 10 different artificial earthquake records, representing a ready-made design spectrum for type II soil. Studies reveal that the estimations made on the nonlinear dynamic response of high-rise structures are more accurate when compared to nonlinear static methods. The effective parameters in the seismic design of the braced steel structures such as the ductility, overstrength and response modification factors in ELBRF are calculated.

2. Elliptic bracing system

SMRF and CBF are usually applied in structures. SMRF is subject to appropriate lateral load generation with respect to structural plasticity. [13] The utility of the structures is constrained when essential parameters like the excessive relative displacement (due to high structure flexibility) are applied and the inevitable stress concentration at the weld columns and beams are sought. The improved stiffness is achieved by applying CBF if the reduction of executive structure deformation is of matter. Adding bracing parts to an SMRF system, as well as implementing such a design would prevent the lower ductility of CBF due to seismic performance factor [14]. By reviewing the available literature on the subject, it is found that bracing members' buckling in CBF is faced with undergoing structural defaults, which promotes energy loss.

ELBRF is a novel system which is originally introduced in 2016 by the authors of this present research [15]. The newly proposed structural form where ELBRF is adopted in the intermediate opening of the frame would cause an increase in design efficiency. In its geometrical sense, an elliptic brace having a broader architecture in its opening is better than concentric bracing. Applying this ELBRF will lead in improving structure behavior and energy dissipation thereof it is advised because its opening space is free of architectural space problem [15-21]. The ductility and overstrength response modification volumes are assessed as well, Figure (1).

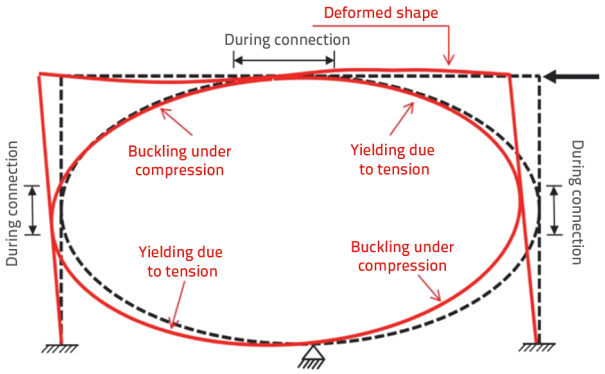

Figure 1. Nonlinear deformation in elliptic bracing [15-21]

In this system, the column and beam connections to the elliptic brace must be clamped as double joints, (i.e. the connections must have sufficient flexural stiffness at the connection point to withstand out-of-plane buckling). The connections of the frame to the elliptical brace have produced the degrees of indeterminacy in the structure so that it has a proper stability. Here, the braces of the truss parts are not perpendicular to the frame plate but behave as the beam-column elements. Bracings under pressure might experience out-of-plane buckling that is caused by generated deformations at beam, and column connection points in the plate frames might occur when the bracings undergo pressure, Figure 1. The braces could be designed and installed in a way that appropriate bracing connections are available on the column and beam, which would provide sufficient stiffness.

In an ELBRF system subjected the lateral load (from left to right), tension and compression forces were produced in each of the elliptical brace's quarter segments. Distribution of the internal forces in the quarter segments of the elliptic brace caused to subject the right-side and left-side columns to the compressive and tensile axial loads, respectively. The mechanism of the structure's in-plane failure was due to the buckling of quarter segments of the elliptic brace under compression and the formation of plastic hinge in the middle of the segments. It is worth noting that this mechanism is based on the assumption of adequate out-of-plane stability of the structure.

3. Nonlinear static procedures for seismic demand estimation

3.1. Load patterns

There are several procedures that could be adopted for conducting a nonlinear static analysis. While the fundamental procedure for the step-by-step analysis is essentially the same, the procedures vary mostly in the form of lateral force distribution applied to the structural model in each step of the analysis. FEMA-356 (2000) [5] and similar references recommend the following procedures: Chosen load patterns are inverted triangular, uniform and mode-one load patterns which are introduced briefly here. Inverted Triangular pattern results in an inverted triangular distribution at the height of the building and is normally valid when the mass participation in the fundamental mode of vibration is more than 75 %. This lateral load pattern is expressed by the following FEMA-356 (2000) [5] equation (1):

$$F_i = \frac{W_i h_i}{\sum_{j=1}^{n} W_j h_j} V \tag{1}$$

where, F_i is the lateral load at floor level i, W_i is the weight at floor level i, h_i is the height from base to floor level i and V is the total lateral load (base shear) to be applied. Uniform load pattern is based on the lateral forces that are proportional to the total mass at each floor level expected to simulate the story shears and is obtained as follows [5]:

$$F_i = \frac{W_i}{\sum_{j=1}^{n} W_j} V \tag{2}$$

Mode-one load pattern is proportional to the fundamental mode of modal responses extracted from the Response Spectrum Analysis (RSA) of the building [5].

3.2. Modal Pushover Analysis (MPA)

Before the pushover analysis is run, the structure is first analyzed while being subjected to gravity loads. These loads are inflicted through a load-controlled static analysis of 10 steps according to [22]. For all the subsequent analyses the structure is subject to their loads. The load Const command (used in resetting the time to zero so that the pushover begins from time zero) is applied after the gravity analysis end. This analysis is run through a displacement-controlled static analysis.
In this article, the structure is pushed up to the target displacement and through the MPA procedure that was introduced by Chopra and Goel (2004) [22].

4. Nonlinear Time History Analysis

4.1. Selection of acceleration scale

Seismic accelerations are selected in NTHAs for SMRFs, X-braced CBFs, Inverted V-Braced CBFs, and ELBRFs frames. Selected ground movement is widely applied in many recent studies representing the structure site which its parameters are depended to the specifications of the site where the structures are built. A detailed description of the features of records set [23] is provided. The 10 records of far-field earthquakes with different magnitudes and distances applied in this study are tabulated in Table 1. These records are extracted from the Pacific Earthquake Engineering Research (PEER) Site. The shear wave velocities of all these sites are classified in type II soil through seismic design code (Standard 2800), [11] and B grouping in USGS site.
Based on International Building Code (IBC), [24] and the California Building Code (CBC), [25], it is required to scale earthquake records in accordance with ASCE 7-05 (2005), [26].
For this purpose, the ground motion is scaled to its maximum gravity acceleration g and the acceleration response spectrum for each one of the measured earth motions is assigned to be 5 % damped. Additionally, they are scaled in a sense that, for each structure with a period T in 0.2T to 1.5T range, the mean value of the Design Response Spectrum shall not be less than 10 % of 1.3 times the corresponding value of the standard spectral design of the standard type II soil plan (T being the building's main alternate period). The spectral design's acceleration in terms of first mode spectral acceleration of the soil type II, while soil is in terms of alternate time periods of the structure (T) and the scaled response spectrum of the earthquake records are illustrated in Figure 2.

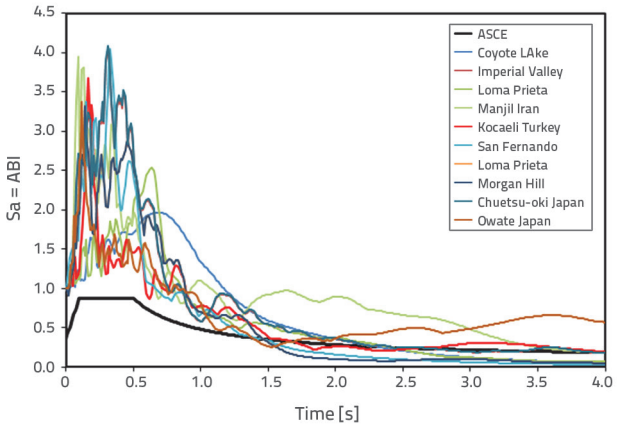

Figure 2. Scaled Response Spectra for each frame

5. The studied models

Four frames including SMRFs, X-Braced CBF, Inverted V-Braced CBF and ELBRF systems are designed according to the requirements of Iranian earthquake resistance design code (Standard 2800) [11] and Iranian National Building code (Part10) [12] in the case of 3, 5, 7, and 10-story steel structures, assumed to be in an area of high seismicity with type II soil and where the average shear wave velocities are of 750-360 m/s² at a depth of 30 m [11].

Table 1. Characteristics of earthquake records used for Nonlinear Time History Analysis

Earthquake	Data	Station	Component [°]	VS30 [m/s]	PGA
Jezero Coyote	06.08.1979.	Gilroy Array	230	663.31	0.422
Coyote Lake	15.10.1979.	Cerro Prieto	E	471.53	0.168
Imperial Valley (EL Centro)	18.10.1989.	BRAN	90	476.54	0.502
Loma Prieta	18.10.1989.	Southwest Abutment	285	561.43	0.485
Loma Prieta	20.06.1990.	Abbar	T	723.95	0.497
Manjil Iran	17.08.1999.	Arcelik	0	523.0	0.210
Kocaeli Turkey	09.02.1971.	Castaic	270	450.28	0.320
San Fernando	24.04.1984.	Brana Anderson (Downstream)	250	488.77	0.422
Morgan Hill	16.07.2007.	Yamakoshi Takezawa Nagaoka	NS	655.45	0.356
Chuetsu - Oki Japan	13.06.2008.	Tamati Ono	NS	561.59	0.285
Iwate Japan					

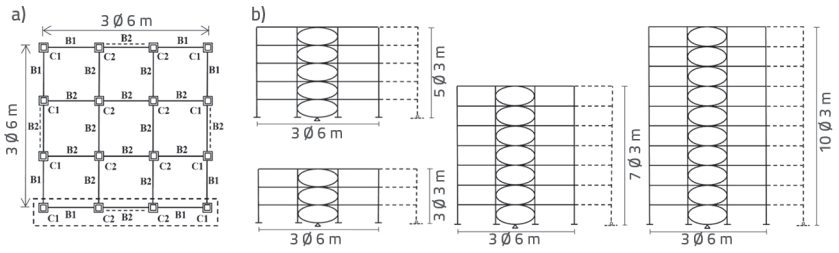

Figure 3. The configuration of the model structure by Open Sees: a) Plane; b) Brace configuration with dummy column

All the stories have a height of three meters and three spans in each story with the length of six meters. The mid-span of the frames is braced. The location of the braces is presented in dotted line in Figure (3). The weight effects of the other frames are modeled by a dummy column, (Figure 3). Type ST37-1 steel (equal to S235 steel based on EN 10025 standard) and a yield stress of 235 MPa is used. The dead and live loads are equal to 5.0 and 2.0 KN/m^2, respectively. All connections of the columns to beams and braces thereof are clamped. All columns support is clamped such that any translational and rotational degree of freedom remains constant. The occurrence of supporting conditions, if any, is expected in the middle of the frames beneath the elliptic bracings in pinned restraint case.

In designing the SMRF, X-Braced CBF, Inverted V-Braced CBF, and ELBRF the equivalent static lateral forces on all the stories are applied subject to earthquake effect. These forces are calculated following the Iranian Earthquake regulations (Standard 2800) [11]:

$$V = C \cdot W = \left[\frac{A \times B \times I}{R}\right] \cdot W \tag{3}$$

where V is the base shear, C is the seismic coefficient, W is the effective structural weight, A is the design base acceleration, B is the response factor, I is the importance rate and R is the response modification factor (behavior ratio). In this calculation, A and I of the frames are 0.35 and 1, respectively.

In ultimate limit state design method is 7.5, 7.0, 7.0 and 9.0, respectively constitute the response modification factor for SMRF, X-Braced CBF, Inverted V-Braced CBF, and ELBRF. Load and Resistance Factor Design (LRFD) has applied some parts of the frame design based on the Iranian National Building Code (part 10) for steel structure design [12]. According to Table 2, IPE section is applied in beam section and Box section are chosen for columns and braces design. By selecting a 2D frame as a representative of a 3D frame the time and volume of the calculations in NTHAs and NSPA would reduce.

6. OpenSees software

To conduct NSPA and NTHAs on the structure, OPENSEES 2.4.6 [27] software has been applied. This software is developed by Berkeley University of California, a very practical software for nonlinear and dynamic analyses.

Nonlinear beam-column elements are applied to model the columns, beams, and elliptic bracings. These elements could consider P-Δ effects and large deformations in a given nonlinear geometry effect of the model. In order to expand the model plasticity along the part length and nonlinear buckling, each one of the elements is divided into several strings, then into the cross-sections and several sections in their lengths, Figure 4. To increase the accuracy of the analysis, the beam and column elements are proportioned into 10 and the elliptic bracing is proportioned into 32 with which each are of the openings. The steel section flange and web applied in the model is proportioned into 15-to-20 strain elements along the flange and web based on their dimensions.

The 3-D structures are designed in ETABS environment. The selected 2-D frames are modeled in a 3-D in OpenSees 2.4.6 environment [27]. Structures, loadings, and earthquake forces are considered in an plate in 2-D and the degrees of freedom of all the nodes except those of the bracings are fixed in the -direction. In this setup, braces could buckle out their plates. In order to model out-of-the-plane buckling, the initial imperfection is considered to be 0.0015 for the bracings; and owing to the elliptic bracing being curved, there is no need to assign the initial imperfection inside-of-the-plane buckling within the plates.

The initial imperfection is assigned to all the columns at the mid-length in order to apply the nonlinear geometrical aspects [28]. The masses of the stories are set according to the rigid diaphragm for dynamic analysis, then the array section is applied for each one of the members. The effect of the weight of other frames are modeled through a dummy column.

To model the P-Δ effect of adjacent gravity frames, a dummy column is applied which is connected to the mainframe's truss elements. This dummy column having an inertia moment and cross-section of which is 100 times greater than the mainframe columns is applied to determine the P-Δ effect of half of the gravity columns of the 3-D structure [29].

Large deformations and the effect of second-order analysis on columns (P-delta) and beams (linear) are determined through a corotational coordinate conversion. In this study, the flexibility of foundation is ignored, and the bottom of the columns are modeled to be clamped. To model a rigid diaphragm, the horizontal displacement of all nodes in a story is tightened to the first left node on the same story in accordance with the equalDOF command. As for half of the total mass of each story, it is assigned to 2-D frame nodes at the same story.

The steel behavior of uniaxial hysteretic materials model is capable to withstand the 3 linear forms of tension and compression behavior. This model is applied to steel components. The stiffness slope of steel subject to tension is observed at 2 % of the elastic area. The behavior model of materials is shown in Figure 5. In this modeling, the P-delta effects and large nonlinear geometric deformations are assigned to geometric stiffness matrix through the corotational deformation [27].

Table 2. Cross sections of models' members

Frame		SMRF			Invent V - Braced CBF			
Structures	Story	C1	C2	B1 i B2	C1	C2	B1 i B2	Vez
3 - Story	1	BOX 200×20	BOX 200×20	IPE 360	BOX 150×15	BOX 150×15	IPE 300	BOX 100×10
	2	BOX 200×20	BOX 200×20	IPE 360	BOX 150×15	BOX 150×10	IPE 300	BOX 100×10
	3	BOX 150×25	BOX 150×25	IPE 330	BOX 150×15	BOX 150×10	IPE 300	BOX 100×10
5 - Story	1	BOX 250×20	BOX 250×20	IPE 400	BOX 150×20	BOX 150×20	IPE 330	BOX 100×10
	2	BOX 250×20	BOX 250×20	IPE 400	BOX 150×20	BOX 150×20	IPE 330	BOX 100×10
	3	BOX 250×20	BOX 250×20	IPE 360	BOX 150×20	BOX 150×15	IPE 300	BOX 100×10
	4	BOX 200×20	BOX 200×25	IPE 360	BOX 150×20	BOX 150×10	IPE 300	BOX 100×10
	5	BOX 200×20	BOX 200×20	IPE 330	BOX 150×20	BOX 150×10	IPE 300	BOX 100×10
7 - Story	1	BOX 350×30	BOX 350×30	IPE 400	BOX 200×20	BOX 200×25	IPE 330	BOX 120×10
	2	BOX 350×30	BOX 350×30	IPE 400	BOX 200×20	BOX 200×20	IPE 330	BOX 120×10
	3	BOX 350×30	BOX 350×30	IPE 400	BOX 150×20	BOX 150×20	IPE 330	BOX 100×10
	4	BOX 350×30	BOX 350×30	IPE 400	BOX 150×20	BOX 150×20	IPE 330	BOX 100×10
	5	BOX 300×30	BOX 350×30	IPE 360	BOX 150×15	BOX 150×15	IPE 330	BOX 100×10
	6	BOX 250×20	BOX 250×20	IPE 360	BOX 150×10	BOX 150×10	IPE 330	BOX 100×10
	7	BOX 200×20	BOX 200×20	IPE 330	BOX 150×10	BOX 150×10	IPE 330	BOX 100×10
10 - Story	1	BOX 450×30	BOX 450×30	IPE 450	BOX 200×20	BOX 250×25	IPE 360	BOX 120×12
	2	BOX 450×30	BOX 450×30	IPE 450	BOX 200×20	BOX 250×20	IPE 360	BOX 120×12
	3	BOX 450×30	BOX 450×30	IPE 450	BOX 200×20	BOX 250×20	IPE 360	BOX 100×10
	4	BOX 450×30	BOX 450×30	IPE 400	BOX 150×25	BOX 200×20	IPE 360	BOX 100×10
	5	BOX 450×30	BOX 450×30	IPE 400	BOX 150×25	BOX 200×20	IPE 330	BOX 100×10
	6	BOX 400×30	BOX 400×30	IPE 400	BOX 150×25	BOX 150×25	IPE 330	BOX 100×10
	7	BOX 400×30	BOX 400×30	IPE 360	BOX 150×25	BOX 150×25	IPE 330	BOX 100×10
	8	BOX 350×30	BOX 350×30	IPE 360	BOX 150×20	BOX 150×20	IPE 330	BOX 100×10
	9	BOX 200×20	BOX 250×25	IPE 330	BOX 150×20	BOX 150×20	IPE 330	BOX 100×10
		BOX 200×20	BOX 200×20	IPE 330	BOX 150×10	BOX 150×10	IPE 330	BOX 100×10

Frame		X- Braced CBF				ELBRF			
Structures	Story	C1	C2	B1 i B2	Ukruta	C1	C2	B1 i B2	Ukruta
3 - Story	1	BOX 150×10	BOX 150×10	IPE 330	BOX 100×10	BOX 200×20	BOX 200×20	IPE 360	BOX 100×10
	2	BOX 150×10	BOX 150×10	IPE 330	BOX 100×10	BOX 150×15	BOX 200×20	IPE 360	BOX 100×10
	3	BOX 150×10	BOX 150×10	IPE 330	BOX 100×10	BOX 150×15	BOX 150×10	IPE 330	BOX 100×10
5 - Story	1	BOX 150×20	BOX 150×20	IPE 330	BOX 100×10	BOX 200×20	BOX 200×20	IPE 330	BOX 100×10
	2	BOX 150×20	BOX 150×15	IPE 330	BOX 100×10	BOX 200×20	BOX 200×20	IPE 330	BOX 100×10
	3	BOX 150×20	BOX 150×10	IPE 330	BOX 100×10	BOX 200×20	BOX 250×20	IPE 330	BOX 100×10
	4	BOX 150×20	BOX 150×10	IPE 330	BOX 100×10	BOX 150×20	BOX 150×20	IPE 330	BOX 100×10
	5	BOX 150×20	BOX 150×10	IPE 330	BOX 80×8	BOX 150×10	BOX 150×10	IPE 330	BOX 100×10
7 - Story	1	BOX 200×20	BOX 200×25	IPE 330	BOX 100×10	BOX 250×20	BOX 250×20	IPE 400	BOX 120×12
	2	BOX 200×20	BOX 200×20	IPE 330	BOX 100×10	BOX 250×20	BOX 250×20	IPE 400	BOX 120×12
	3	BOX 150×20	BOX 150×20	IPE 330	BOX 100×10	BOX 250×20	BOX 250×20	IPE 400	BOX 120×12
	4	BOX 150×20	BOX 150×20	IPE 330	BOX 100×10	BOX 250×20	BOX 250×20	IPE 360	BOX 120×12
	5	BOX 150×15	BOX 150×15	IPE 330	BOX 100×10	BOX 200×20	BOX 200×20	IPE 360	BOX 100×10
	6	BOX 150×10	BOX 150×10	IPE 330	BOX 100×10	BOX 200×20	BOX 200×20	IPE 330	BOX 100×10
	7	BOX 150×10	BOX 150×10	IPE 330	BOX 80×8	BOX 200×20	BOX 200×20	IPE 330	BOX 100×10
10 - Story	1	BOX 200×20	BOX 300×20	IPE 330	BOX 120×12	BOX 350×30	BOX 350×30	IPE 450	BOX 120×12
	2	BOX 200×20	BOX 250×20	IPE 330	BOX 120×12	BOX 350×30	BOX 350×30	IPE 450	BOX 120×12
	3	BOX 200×20	BOX 200×25	IPE 330	BOX 120×12	BOX 350×30	BOX 350×30	IPE 400	BOX 120×12
	4	BOX 200×20	BOX 200×20	IPE 330	BOX 100×10	BOX 350×30	BOX 350×30	IPE 400	BOX 120×12
	5	BOX 200×20	BOX 200×20	IPE 330	BOX 100×10	BOX 350×30	BOX 350×30	IPE 400	BOX 120×12
	6	BOX 150×20	BOX 150×20	IPE 330	BOX 100×10	BOX 250×25	BOX 250×25	IPE 400	BOX 120×12
	7	BOX 150×20	BOX 150×20	IPE 330	BOX 100×10	BOX 250×25	BOX 250×25	IPE 360	BOX 100×10
	8	BOX 150×20	BOX 150×20	IPE 330	BOX 100×10	BOX 200×20	BOX 200×20	IPE 360	BOX 100×10
	9	BOX 150×10	BOX 150×10	IPE 330	BOX 100×10	BOX 200×20	BOX 200×20	IPE 330	BOX 100×10
		BOX 150×10	BOX 150×10	IPE 330	BOX 100×10	BOX 200×20	BOX 200×20	IPE 330	BOX 100×10

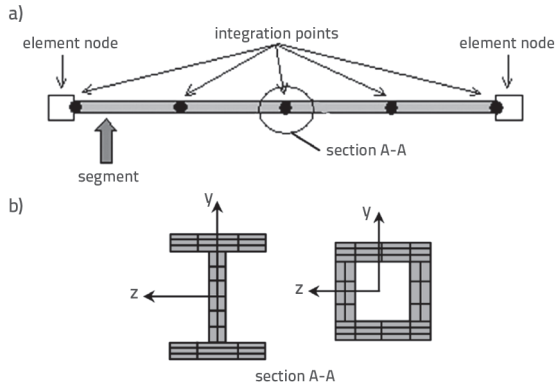

Figure 4. Schematic division of element and section into segment and fiber elements in OpenSees: a) Dividing the element into several segments; b) Dividing the section into fiber elements [27]

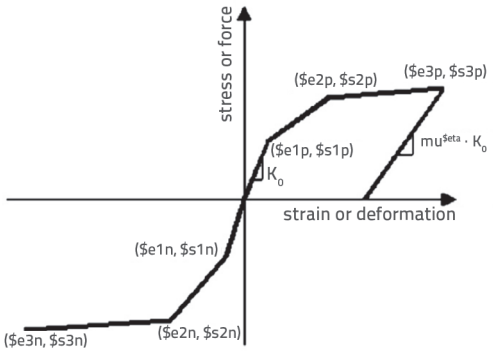

Figure 5. The behavior of hysteric material model [27]

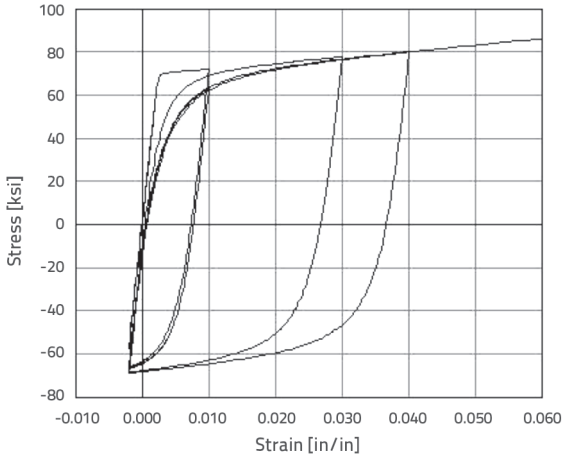

Figure 6. The behavior of material model Steel02 [27]

To model bracing elements in X-Braced CBF and Inverted V-Braced CBF concentrically braced frames, the bracing member is considered with a wide plasticity and the force-based elements with fiber sections are applied in a concentric manner as shown in Figure 4. The P-delta effects and nonlinear geometric deformations are considered through the corotational deformation of the geometric stiffness matrix type in the modeling [30]. A nonlinear beam-column element is applied to model braces as well as to assign the effects of moderate to large deformations caused by to nonlinear buckling of the members. In order to increase the accuracy of the analysis in modeling the structure, five integration points are assigned to the model. Bracing members in Braced CBF and Inverted V-Braced CBF structures are of two sections and the initial defect is set to 0.002 member mid-length in order to determine the nonlinear geometric effects. The applied steel here is of Steel02, Figure 6. To model the steel rapture, the strains are limited by applying MinMax materials, and the tensile strength of the steel makes up 2 % of the elastic zone.

7. The analytical results

7.1. Nonlinear static analysis

After the non-linear static analysis, the Roof displacement-base shear diagrams (that are related to the ELBRF for 3, 5, 7 and 10-story structures) are plotted through the outputs obtained

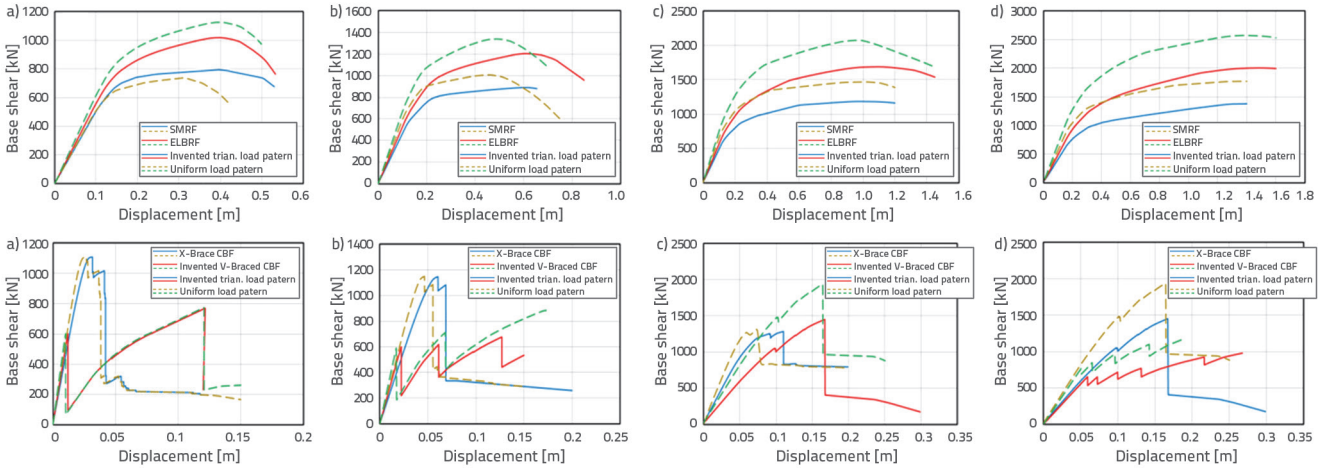

Figure 7. Pushover curves of studied frames in SMRF, X- Braced CBF, Invented V- Braced CBF and ELBRF in: a) 3-Story, b) 5-Story, c) 7-Story, d) 10-Story

Table 3. Overstrength, ductility factors and response modification factor of model for Invented triangular and Uniform load patterns in ELBRFs

No. of story	Invented triangular load pattern						Uniform load pattern					
	R_{SO}	R_S	R_μ	γ	R_{ASD}	R_{LRFD}	R_{SO}	R_S	R_μ	γ	R_{ASD}	R_{LRFD}
3	2.28	2.62	5.1	1.44	19.26	13.37	2.32	2.668	5.24	1.44	20.13	13.98
5	2.1	2.42	4.36	1.44	15.16	10.53	2.17	2.495	4.47	1.44	16.06	11.15
7	2.0	2.30	3.4	1.44	11.26	7.82	2.12	2.438	3.72	1.44	13.06	9.07
10	2.0	2.30	2.97	1.44	9.84	6.83	2.10	2.415	3.14	1.44	10.92	7.58

from OpenSees [27] for the inverted triangular and the uniform load patterns. This plotted scheme is compared with SMRFs, X-Braced CBF and Inverted V-Braced CBF concentrically braced frames as seen in Figure 7.

According to the obtained results above and the description of the design method through the ultimate limit state and allowable stress methods of [31], the ductility, overstrength factors, and response modification factor are calculated through a bilinear ideal curve (Idealized Response).

The primary frames are designed in accordance with the preliminary response modification factor, followed by their empirical values after being evaluated. Therefore, response modification factor was estimated by a try-and-error iterative procedure. To calculate the final response modification factor, the models were modified, assigned and based on this newly modified respond factors, the results are presented in Table 3. As it is clear in this table, overstrength, ductility and response modification factors were decreased by increasing of the frame height. it can be concluded that response modification factor was depended to the configuration of the braces. Although, the elastic stiffness in X-braced CBF and inverted V-braced CBF steel frames was larger than ELBRF system, it was observed that overstrength, ductility and response modification factors in ELBRF system were larger than their corresponding values in other systems. Moreover, by comparing the variation of overstrength and ductility factors in ELBRF system, it is shown that the ductility factor was decreased by increasing the number of stories with a higher rate than overstrength factor..

7.2. Evaluation of conventional pushover procedures

The conventional pushover methods are evaluated by comparing the estimated roof drift ratio (maximum roof displacement normalized by building height), the inter-story drift ratio (relative drift between two consecutive stories normalized by story height), and the story shear values in relation to the nonlinear time history analysis. The time history analysis results are presented in a set of 10 scaled records together with both the mean NTHA and four load patterns in, Figure 8-19.

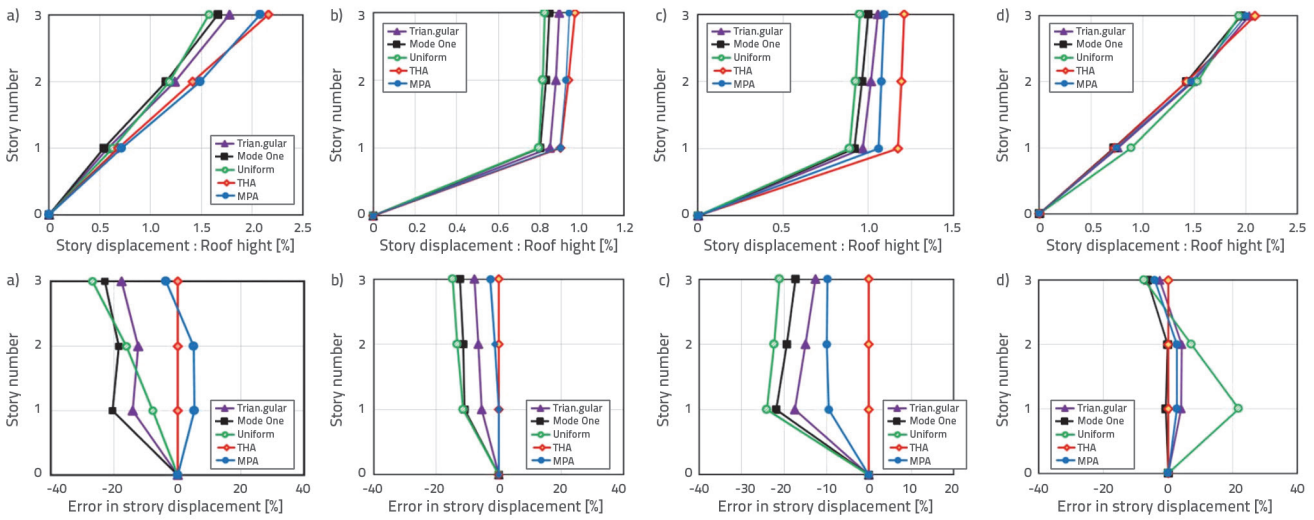

Figure 8. Predicted peak displacement demands and error accrued by NSPs compared to NTH analyses for 3-Story Frames in: a) SMRF; b) X-braced CBF; c) Invented V-braced CBF; d) ELBRF

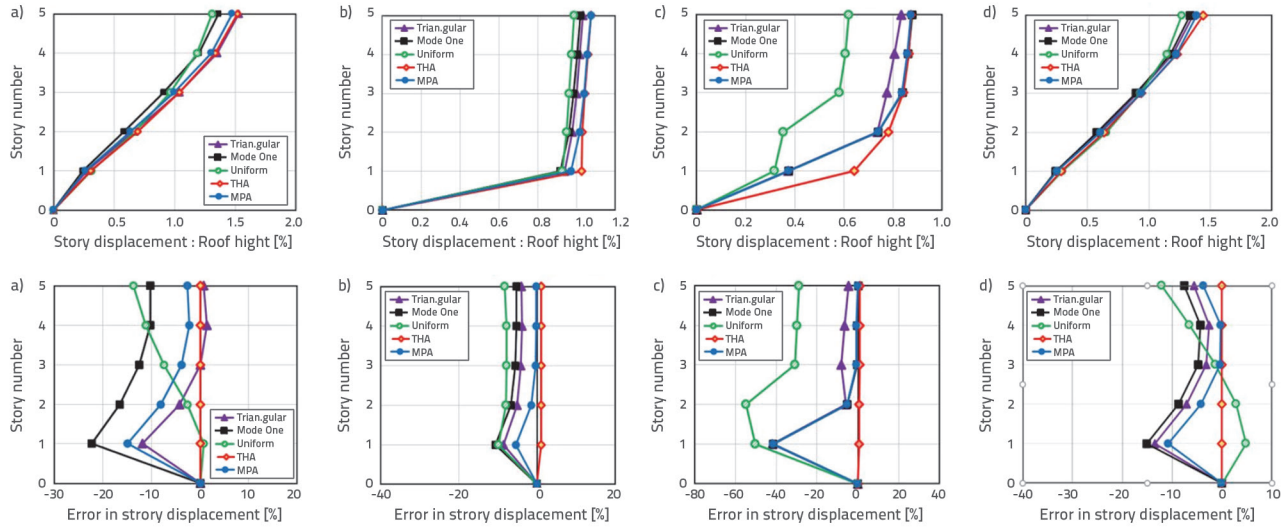

Figure 9. Predicted peak displacement demands and error accrued by NSPs compared to NTH analyses for 5-Story Frames in: a) SMRF; b) X-braced CBF; c) Invented V-braced CBF; d) ELBRF

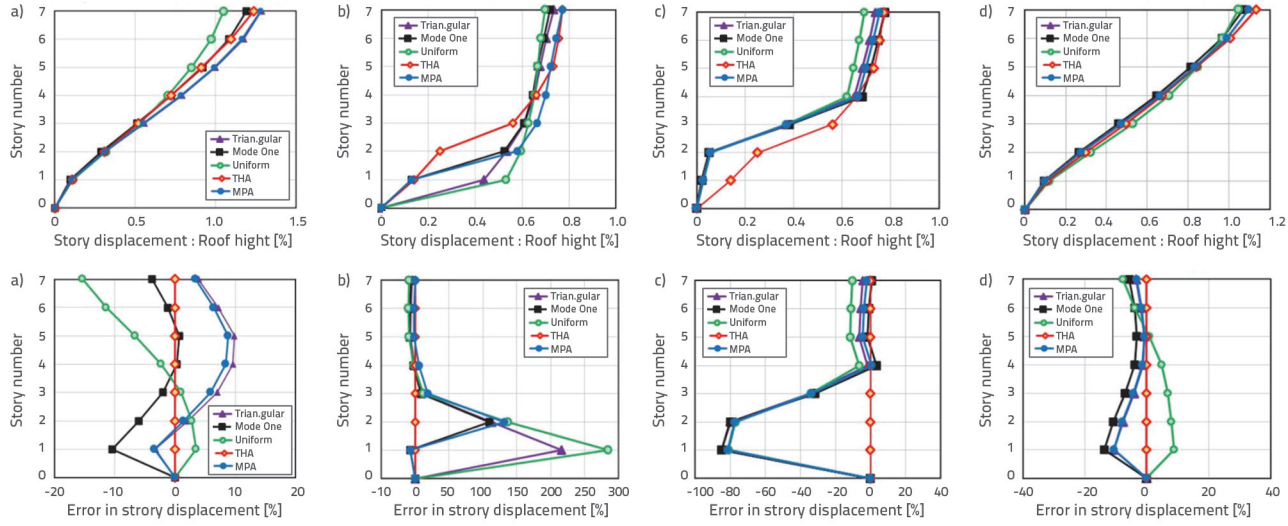

Figure 10. Predicted peak displacement demands and error accrued by NSPs compared to NTH analyses for 7-Story Frames in: a) SMRF; b) X-braced CBF; c) Invented V-braced CBF; d) ELBRF

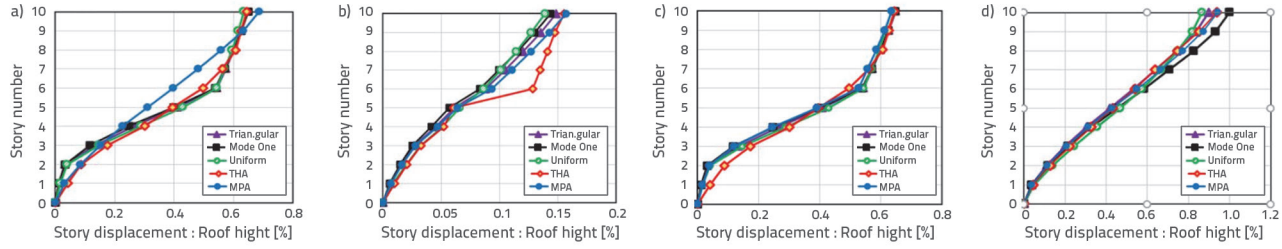

Figure 11. Predicted peak displacement demands and error accrued by NSPs compared to NTH analyses for 10-Story Frames in: a) SMRF; b) X-braced CBF; c) Invented V-braced CBF; d) ELBRF (the first part of the figure)

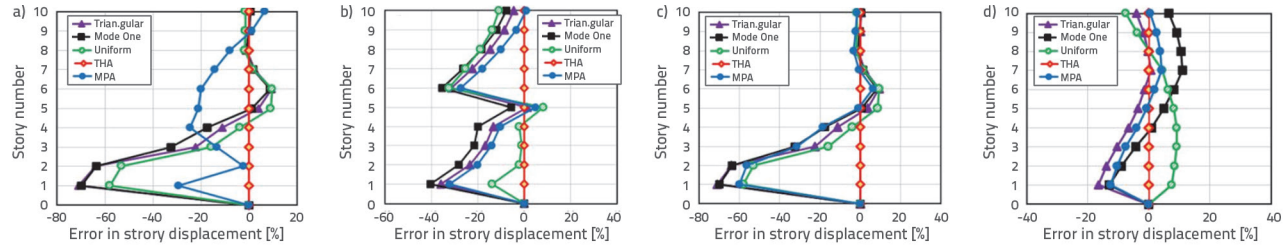

Figure 11. Predicted peak displacement demands and error accrued by NSPs compared to NTH analyses for 10-Story Frames in: a) SMRF; b) X-braced CBF; c) Invented V-braced CBF; d) ELBRF (continuation of the figure)

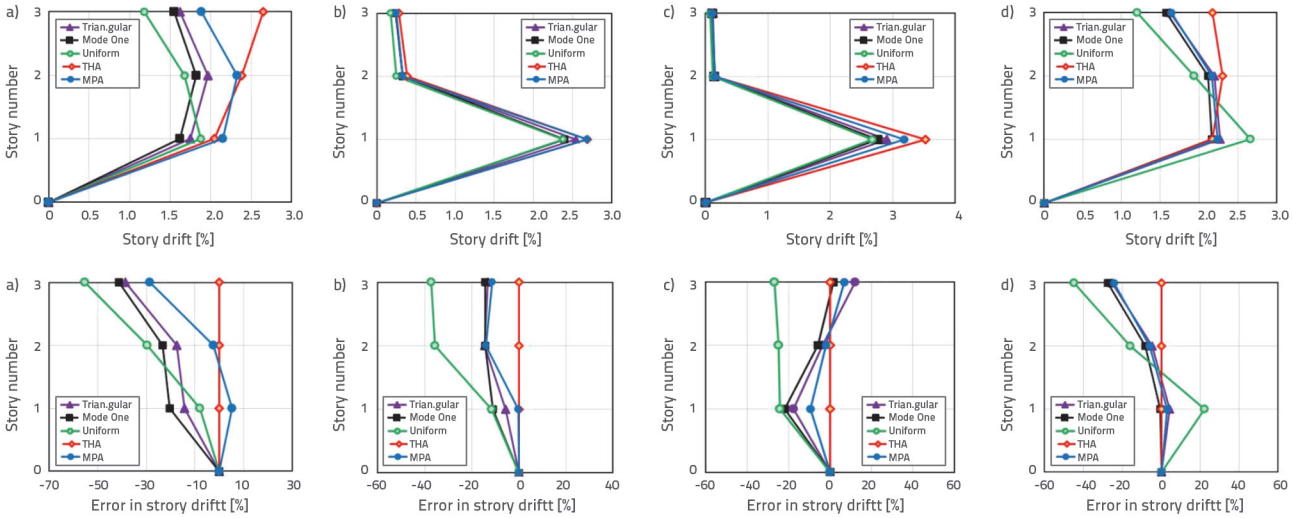

Figure 12. Predicted peak inter-story drift demands and error accrued by NSPs compared to NTH analyses for 3-Story Frames in: a) SMRF; b) X-braced CBF; c) Invented V-braced CBF; d) ELBRF

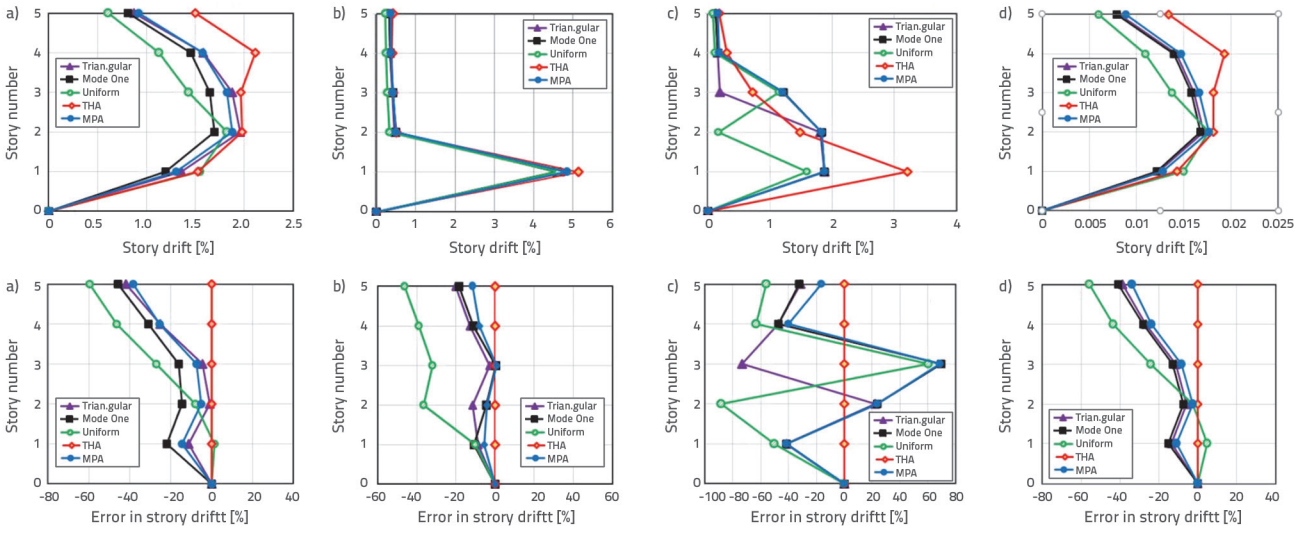

Figure 13. Predicted peak inter-story drift demands and error accrued by NSPs compared to NTH analyses for 5-Story Frames in: a) SMRF; b) X-braced CBF; c) Invented V-braced CBF; d) ELBRF

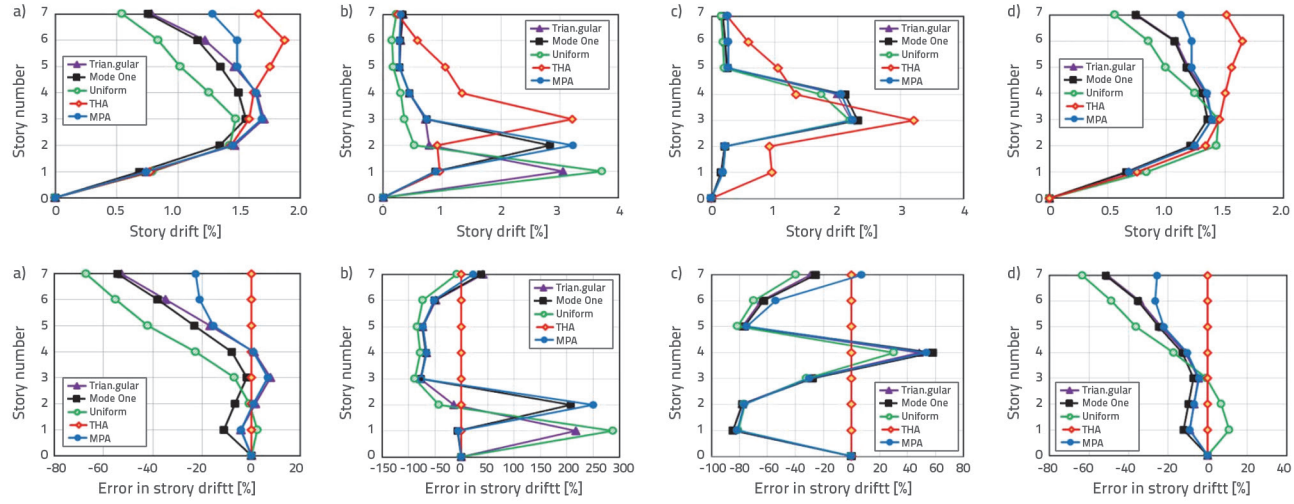

Figure 14. Predicted peak inter-story drift demands and error accrued by NSPs compared to NTH analyses for 7-Story Frames in: a) SMRF; b) X-braced CBF; c) Invented V-braced CBF; d) ELBRF

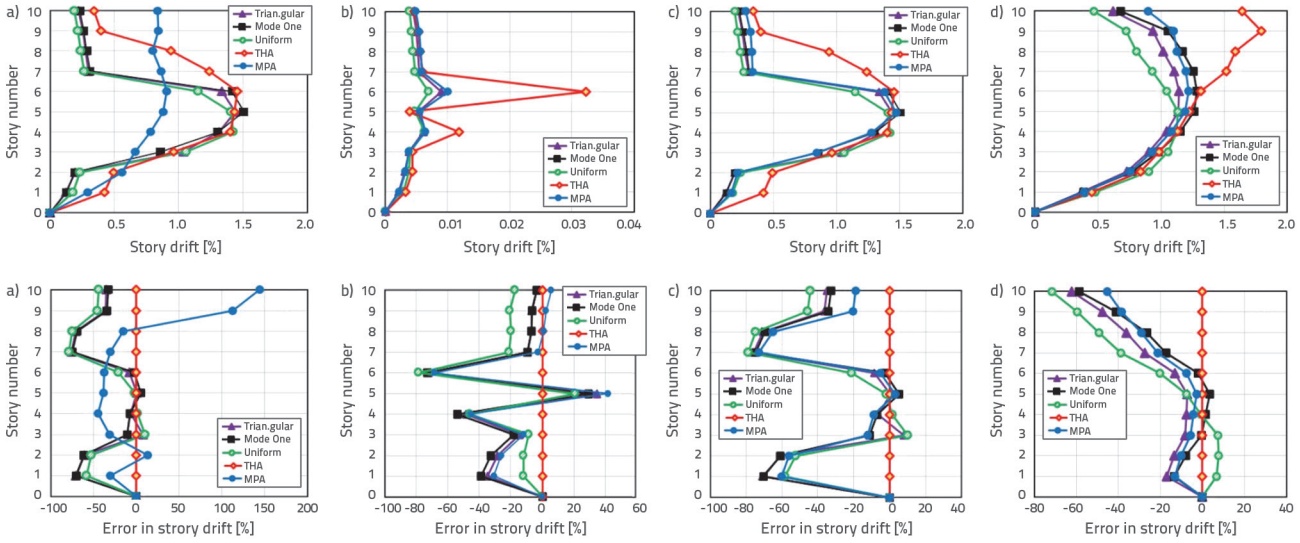

Figure 15. Predicted peak inter-story drift demands and error accrued by NSPs compared to NTH analyses for 10-Story Frames in a) SMRF, b) X-braced CBF, c) Invented V-braced CBF and d) ELBRF

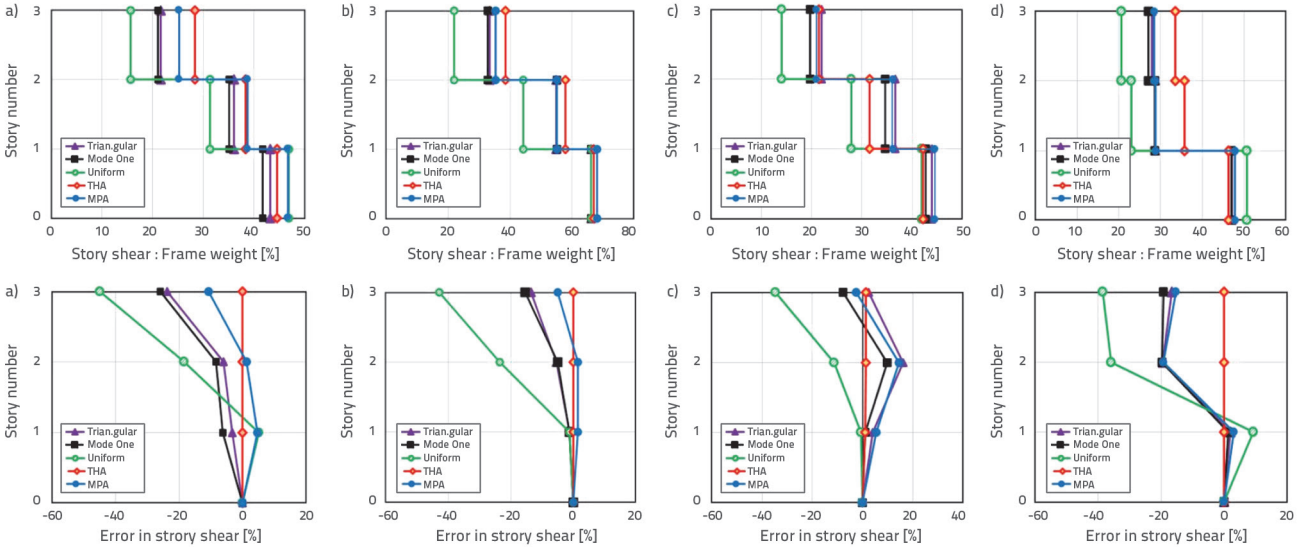

Figure 16. Predicted Shear Story and error accrued by NSPs compared to NTH analyses for 3-Story Frames in: a) SMRF; b) X-braced CBF; c) Invented V-braced CBF; d) ELBRF

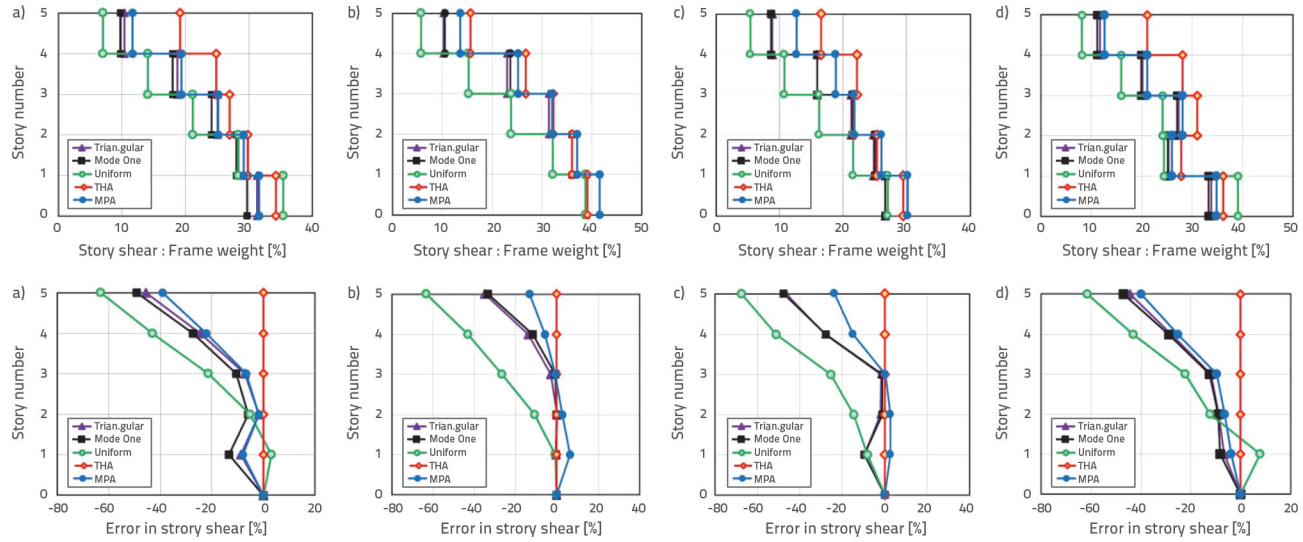

Figure 17. Predicted Shear Story and error accrued by NSPs compared to NTH analyses for 5-Story Frames in: a) SMRF; b) X-braced CBF; c) Invented V-braced CBF; d) ELBRF

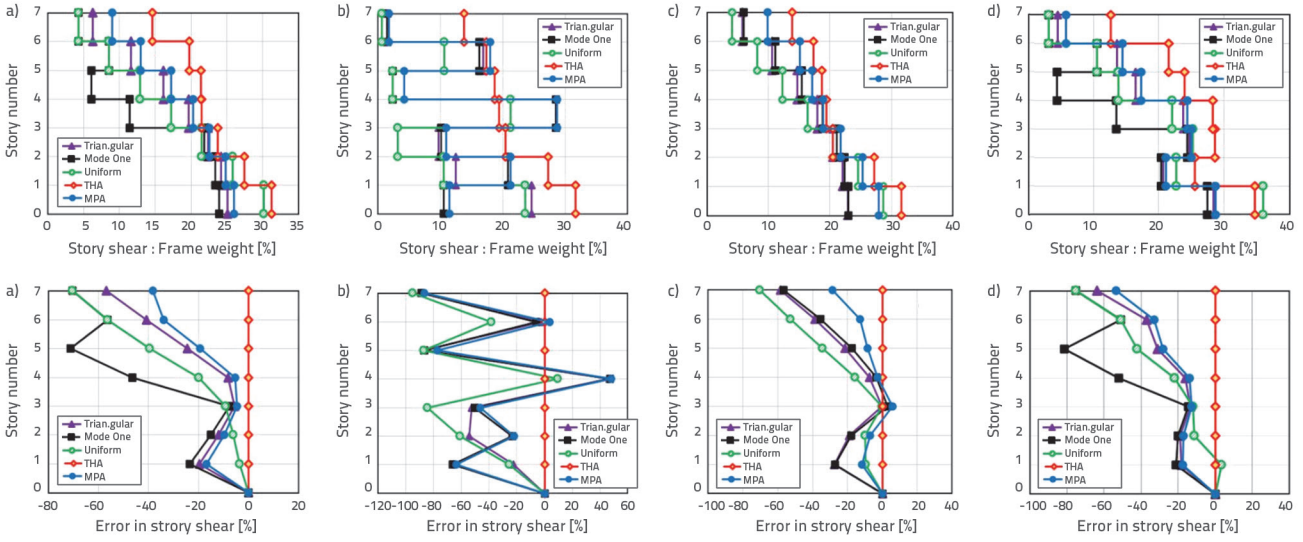

Figure 18. Predicted Shear Story and error accrued by NSPs compared to NTH analyses for 7-Story Frames in: a) SMRF; b) X-braced CBF; c) Invented V-braced CBF; d) ELBRF

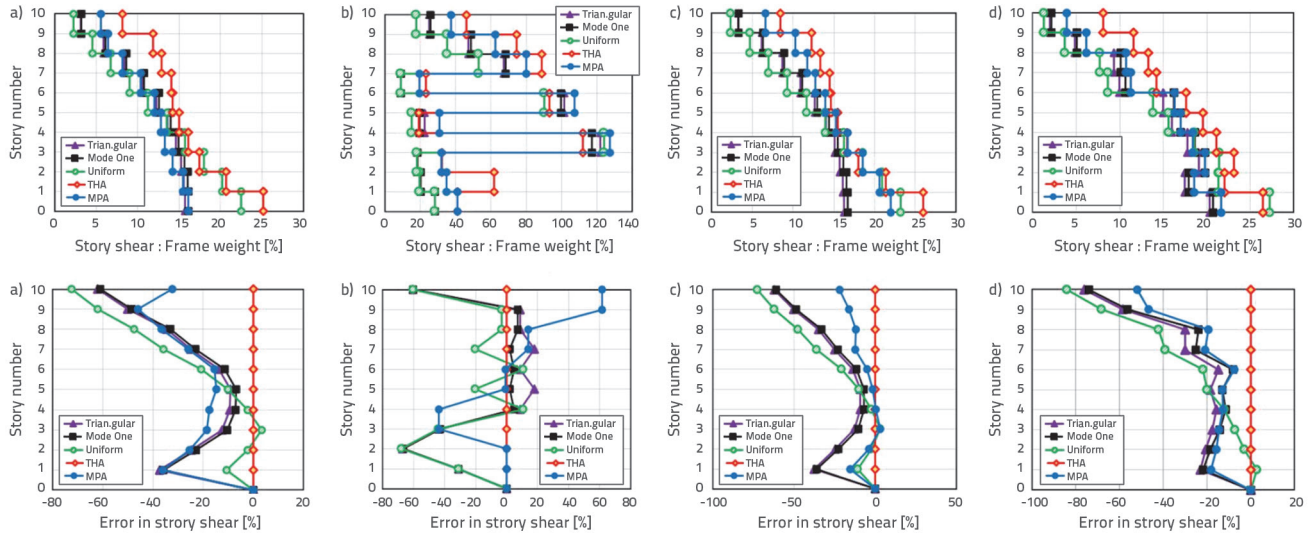

19. Predicted Shear Story and error accrued by NSPs compared to NTH analyses for 10-Story Frames in: a) SMRF; b) X-braced CBF; c) Invented V-braced CBF; d) ELBRF

In this article, the floor displacements, story drift ratios, and story shear are all estimated by referring to ELBRFs through conventional nonlinear static pushover analyses. Maximum floor displacement is estimated by the uniform load pattern for 7 and 10-story ELBRF accurately, while this method is not applicable for the estimation of the inter-story demand for a similar model. However, the modal Pushover Analysis (MPA) method, with respect to involved higher modes of the structure, is an accurate method for estimating the story shear demand of the 7 and 10-story ELBRF model. In addition, this method is very accurate for estimating the inter-story drift of the ELBRF-7 and 10-story ELBRF model. In general, if the objective is to estimate floor displacements, story drift ratios, and story shear for 7 and 10-story ELBRF, among the proposed methods the Modal Pushover Analysis (MPA) is deemed the best.

Maximum floor displacement is estimated through a relative accuracy with a uniform load pattern for the 5 story ELBRF model. However, this loading pattern is not a suitable method for estimating inter-story drift and story shear for both 3 and 5-story ELBRF models. Therefore, adoption of Single Run SSP or Modal Pushover Analysis (MPA) methods is recommended since as observed, the Modal Pushover Analysis (MPA) is a relatively accurate method adopted in estimating high-rise ELBRF seismic performance.

The accuracy of conventional nonlinear static methods adopted in estimating the seismic requirements of ELBRF structures, while using 10 high-intensity ground motion records are assessed through the bulleted conclusion below. These conclusions are based on a comparison of NSPA estimates of seismic demands and the determination of the corresponding values obtained through NTHA for 3, 5, 7 and 10-story ELBRF structures, designed with the standards of the earthquake regulations:

The equivalent bilinear SDF systems for the 7 and 10-story ELBRF determined through non-linear static methods can estimate the peak roof displacement in a perfectly accurate manner compared to the peak roof displacement in NTHA method, but this system is of no efficiency in 3 and 5-story ELBRF models.

The Story drift requirements are calculated through Single Run SSP and three other conventional load patterns in accordance with the NTHA results. Extraction of higher modes through MPA method in response to 3 and 5-storey ELBR buildings, in general are of no statistical significance, that is, the first mode by itself may be sufficient for load pattern of one mode at low and mid-rise ELBRFs.

The precision of all proposed steps in estimating the maximum story drift and roof displacement in low and mid-rise modes in all classes is generally low. However, the precision of these methods in estimating the peak story drift of an individual story can be applied in specific cases. All of the adopted procedures yield almost similar results in practice, but, the Uniform Load Pattern is slightly simpler and more practical than other load patterns.

7.3. The error prediction of total model

In order to compare the accuracy of different NSPs parameters in ELBRF, the following error index used by [31] is applied in this study. The results obtained for ELBRF frames are exhibited in Figure 20 in bar-chart.

$$ERROR_{(NSPS)} = 100 \times \sqrt{\left(\frac{1}{n}\right) \times \sum_{i=q}^{n} \left(\frac{NSP_{Parameters} - THA_{Parameters}}{THA_{Parameters}} \right)^2} \quad (4)$$

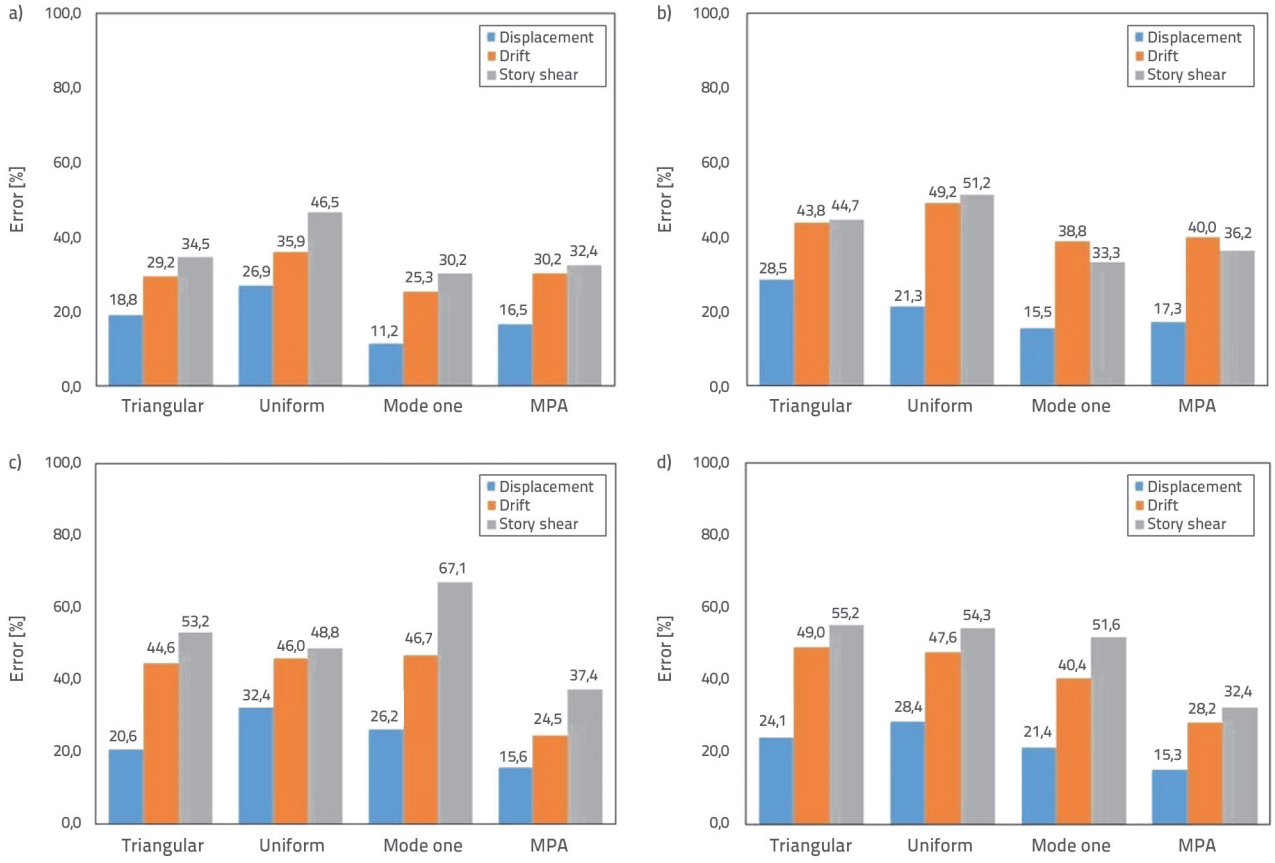

Figure 20. Comparison of the accuracy of the different NSPs parameters for: a) 3-Story; b) 5-Story; of ELBRF building; c) 7-Story; d) 10-Story of ELBRF building, using an error index defined by Eq. (4)

8. Conclusion

The ductility, overstrength factors, response modification factor and the process of forming plastic hinges for ELBRF are all evaluated subject to the inverted triangular load pattern and uniform load pattern by running nonlinear static analysis. According to the diagrams drawn based on conventional pushover methods, comparing the estimated roof drift ratio (maximum displacement of the normalized roof with the height of the building), the inter-story drift ratio (relative drift between the two consecutive classes normalized to the floor height) and the story shear values, results are briefed in bullets as follows:

- The overstrength factor for ELBRF subject to the inverted triangle and uniform load patterns are 2.4 and 2.5, respectively.
- The ductility factor for ELBRF subject to the inverted triangle and uniform load patterns are 4.0 and 4.15, respectively.
- In general, the overstrength factor and the force reduction factor derived from ductility for the ELBRF are recommended as 2.45 and 4.1, respectively.
- The response modification factor for ELBRF is proposed for both design methods (ultimate limit state and allowable stress methods) as 10 and 14.4, respectively.
- Overstrength and ductility factors decrease with an increase in the number of stories.
- Both the X-braced and Inverted V-Braced CBFs do not have an appropriate drift distribution at building heights, except in one or two stories where they are of high drift. The story drift distribution in SMRF structure is more uniform than that of two X-braced CBFs and Inverted V-braced CBFs structures, indicating that the stories reach a certain drift rate with one another. The drift distribution of the ELBRF structure is better than SMRF, and in 3, 5 and 7-story ELBRF structures, this distribution is more uniform and lower, indicating an improvement in structure's performance against earthquakes. In a 10-story ELBRF structure, the drift distribution in upper stories is relatively higher than that of the lower stories, indicating the potential of a failure in the upper stories in the high-rise ELBRF structures.
- The displacement values in the lower stories of X-braced CBFs and Inverted V-braced CBFs structures is very high and in the upper stories is almost the same. In the 3, 5 and 7-story SMRF and ELBRF structures, the displacement distribution is linear. However, displacement values in ELBRF structures are less than that of SMRF. Displacement of distribution in

the 10-story ELBRF structure is left linear while the SMRF structure behavior is similar to those of X-braced CBFs and Inverted V-braced CBFs.

- As the number of stories increases, the appropriate base shear to building weight ratio decreases. By converting the structure from SMRF system to the ELBRF, due to the same weight of both structures, the base shear increased randomly. The shear distribution in the middle stories of ELBRF is noticeably greater than that of the SMRF, while, in all ELBRF structures, decreased shear is evident in the second story.

REFERENCES

[1] Krawinkler, H., Seneviratna, G.: Pros and cons of a pushover analysis of seismic performance evaluation, Engineering structures, 20 (1998), pp. 452-464.

[2] Moghaddam, H., Hajirasouliha, I.: An investigation on the accuracy of pushover analysis for estimating the seismic deformation of braced steel frames, Journal of Constructional Steel Research, 62 (2006), pp. 343-351.

[3] Bracci, J.M., Kunnath, S.K., Reinhorn, A.M.: Seismic performance and retrofit evaluation of reinforced concrete structures, Journal of Structural Engineering, 123 (1997), pp. 3-10.

[4] FEMA F 273 NEHRP: Guidelines for the seismic rehabilitation of buildings, Federal Emergency Management Agency, (1997).

[5] FEMA P: Commentary for the seismic rehabilitation of buildings, FEMA-356, Federal Emergency Management Agency, Washington, DC, (2000).

[6] Saravanan, M., Arul, J., Marimuthu, V., Prabha, P.: Advanced analysis of cyclic behaviour of plane steel frames with semi-rigid connections, Steel and Composite Structures, 9 (2009), pp. 381-395.

[7] Gupta, B., Kunnath, S.K.: Adaptive spectra-based pushover procedure for seismic evaluation of structures, Earthquake spectra. 16 (2000), pp. 367-392.

[8] Fajfar, P., Gašperšič, P.: The N2 method for the seismic damage analysis of RC buildings, Earthquake Engineering & Structural Dynamics, 25 (1996), pp. 31-46.

[9] Hsu, H.L., Tsao, J.W.: Flexural–torsional performance of thin-walled steel hollow box columns subjected to a cyclic eccentric load, Thin-walled structures, 45 (2007), pp. 149-158.

[10] Chopra, A.K., Goel, R.K.: A modal pushover analysis procedure for estimating seismic demands for buildings, Earthquake Engineering & Structural Dynamics, 31 (2002), pp. 561-582.

[11] BHRC: Iranian code of practice for seismic resistance design of buildings: standard no. 2800, 4 ed. (Building and Housing Research Center, Tehran (Iran), 2013).

[12] MHUD: Iranian National Building Code, part 10, steel structure design ed. (Ministry of Housing and Urban Development, Tehran (Iran), 2013).

[13] Chou, C.C., Tsai, K.C., Wang, Y.Y., Jao, C.K.: Seismic rehabilitation performance of steel side plate moment connections, Earthquake Engineering & Structural Dynamics, 39 (2010), pp. 23-44.

[14] Longo, A., Montuori, R., Piluso, V.: Plastic design of seismic resistant V-braced frames, Journal of Earthquake Engineering, 12 (2008), pp. 1246-1266.

[15] Ghasemi, J.H., Haghollahi, A., Moghaddam, H., Moghadam, A.S.: 2099. Study of the seismic performance of steel frames in the elliptic bracing, Journal of Vibroengineering, 18 (2016).

[16] Ghasemi, J.H., Haghollahi, A., Moghaddam, H., Moghadam, A. S.: Assessing Seismic Performance of Elliptic Braced Moment Resisting Frame through Pushover Method, J. Rehabilitation in Civil Eng., 7 (2019) 2, pp. 68-85.

[17] Ghasemi, J.H., Haghollahi, A.: Assessing the seismic behavior of Steel Moment Frames equipped by elliptical brace through incremental dynamic analysis (IDA), J. Earth. Eng. and Eng. Vibration, 19 (2020) 2, pp. 435-449.

[18] Ghasemi, J.H., Haghollahi, A.: Experimental study on hysteretic behavior of steel moment frame equipped with elliptical Brace,. J. Steel and Comp. Struct., 34 (2020) 6, pp. 891-907.

[19] Ghasemi, J.H., Haghollahi, A.: Beheshti-Aval S.B.: Experimental study of failure mechanisms in elliptic-braced steel frame, J. Steel and Comp. Struct., 37 (2020) 2, pp. 175-191.

[20] Ghasemi, J.H., Haghollahi, A.: Experimental and analytical study in determining the seismic demand and performance of the ELBRF-E and ELBRF-B braced frames, J. Steel and Comp. Struct., 37 (2020) 5, pp. 571-587.

[21] Ghasemi, J.H., Haghollahi, A., Talebi Kalaleh, M., Beheshti-Aval, S.B.: Nonlinear seismic behavior of elliptic-braced moment resisting frame using equivalent braced frame, J. Steel and Comp. Struct., 40 (2021) 1, pp. 45-64.

[22] Goel, R.K., Chopra, A.K.: Evaluation of modal and FEMA pushover analyses: SAC buildings, Earthquake spectra, 20 (2004), pp. 225-254.

[23] Medina, R.A., Krawinkler, H.: Seismic demands for nondeteriorating frame structures and their dependence on ground motions (Pacific Earthquake Engineering Research Center), 2004.

[24] Code, U. B.: International conference of building officials, Whittier, CA, 2006.

[25] Code, U. B.: International conference of building officials, Whittier, CA, 2007.

[26] Minimum design loads for buildings and other structures, Vol 7 ed. (Amer Society of Civil Engineers, 2005).

[27] Mazzoni, S., McKenna, F., Fenves, G.L.: OpenSees command language manual, Pacific Earthquake Engineering Research (PEER) Center, 264 (2005).

[28] Asgarian, B., Aghakouchack, A., Bea, R.: Inelastic postbuckling and cyclic behavior of tubular braces, Journal of Offshore Mechanics and Arctic Engineering, 127 (2005), pp. 256-262.

[29] Ibarra, L.F., Krawinkler, H.: Global collapse of frame structures under seismic excitations, (Pacific Earthquake Engineering Research Center Berkeley, CA, 2005).

[30] Mazzoni, S., McKenna, F., Scott, M.H., Fenves, G.L., Jeremic, B.: Opensees command language manual, 2013.

[31] Uang, C., Establishing, R.: Factors for Building Seismic Provisions, ASCE J, Struct Eng., 117 (1991).